Characterizing the Induced Microseismicity of the 2019 Utah FORGE Well Stimulation

Patrick Bradshaw, Gesa Petersen and Kristine Pankow

University of Utah Seismograph Stations

Keywords
FORGE, Microseismicity, EGS

ABSTRACT

The Utah Frontier Observatory for Research in Geothermal Energy (FORGE) Project is a Department of Energy funded research facility dedicated to developing the technologies necessary for Enhanced Geothermal System (EGS) production. The induced seismic activity that results from injecting fluid underground is a major obstacle for public acceptance of EGS. This motivates the Utah FORGE investigation into the feasibility of increasing a reservoir's permeability while keeping induced seismicity below nuisance levels. In 2019, FORGE researchers conducted the first of several well stimulations that are planned for the site. The resulting induced seismic activity was continuously recorded on a local-scale surface seismic network, a ~300 meter instrumented borehole (instrumentation includes a collocated 3-component short-period seismometer and a 3-component accelerometer), and a surface nodal geophone array. During times of stimulation, the seismicity was also monitored using a 12-level borehole geophone string. In this study, we utilize an enhanced earthquake catalog for the 2019 stimulation that used matched filters applied to data collected at the ~300 meter borehole. We calculate theoretical maximum magnitudes for an induced event using physics-based and statistics-based approaches and compare the theoretical values to the maximum magnitudes found in the enhanced catalog. We then analyze the total number of events in the sequence together as a function of injected fluid volume and time. Additionally, we conduct first motion analysis of seismic events that were recorded by the nodal geophone array with a high signal-to-noise ratio and compute first motion focal mechanisms. We use the results from these analyses to inform what we expect for the 2022 and future stimulations at FORGE.

1. Introduction

Enhanced geothermal systems (EGS) are created by injecting water into hot, dry subsurface rocks at high pressures to form a reservoir. They have the potential to improve the accessibility of geothermal development and accelerate production in the renewable energy industry. The Utah Frontier Observatory for Research in Geothermal Energy (FORGE) is a Department of Energy funded research facility to develop the requisite technologies needed for EGS production (Moore et al., 2019). One aspect of technology development is microseismic monitoring to both understand reservoir fracture growth and to mitigate potentially damaging and nuisance-level induced seismicity.

To help better inform the Utah FORGE project and seismic monitoring at Utah FORGE a small-scale stimulation in borehole 58-32 (Figure 1) was performed in April 2019 (Moore et al., 2020). The stimulation was divided into three stages that each injected into an isolated zone. Each zone was split into nine cycles in which individual injection experiments were conducted. The first zone stimulated the open-hole from 2240 meters depth to 2293 meters depth using 71 m^3 of fluid. The second zone occurred at the lower portion of the perforated casing from 2123 meters depth to 2126 meters depth and 88 m^3 of fluid were injected. The third zone targeted casing perforated from 2001 to 2004 meters depth. However, the bridge plug that isolated zone 3 from the rest of the well failed. The results of the injection experiments conducted in this zone are thus inconclusive. Seismic monitoring of this stimulation was performed using multiple scales of instrumentation (Pankow et al., 2020). The most complete seismic catalog (435 events, M -2.0 to -0.5) was compiled by Schlumberger using a 12-level geochain deployed to depths of ~1000 meters in borehole 78-32 (Figure 1). Processing by Schlumberger only occurred during active injection phases so no events were recorded in the intermission between stages.

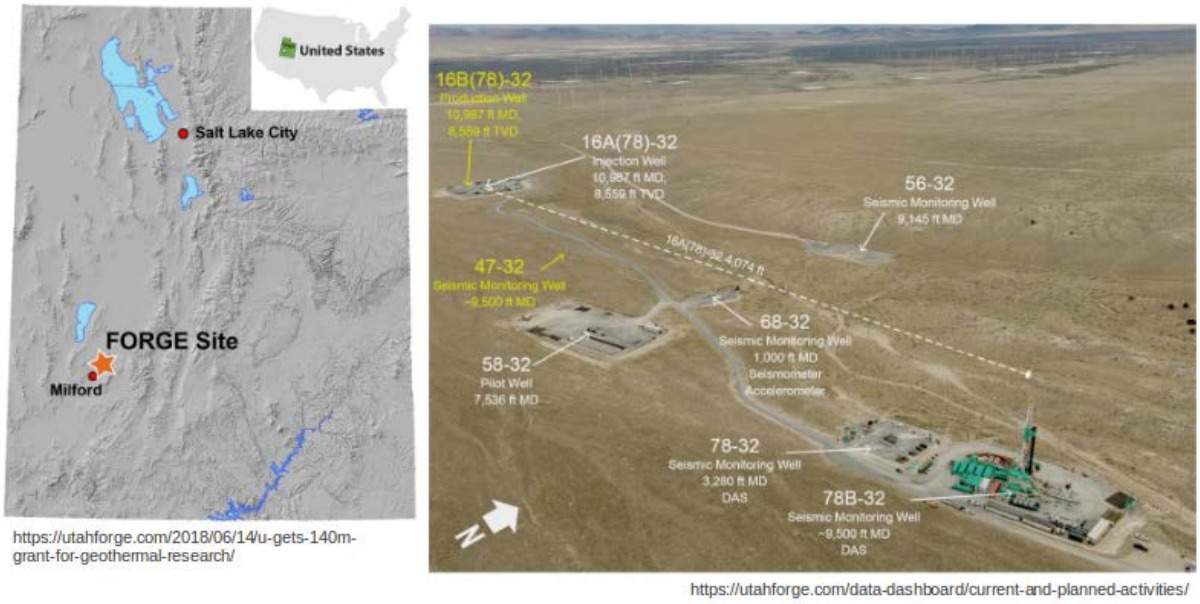

Figure 1: Left, the Utah FORGE site is located ~260 kilometers south of Salt Lake City, UT. Right, location of existing boreholes (white) and planned boreholes (yellow). White dashed line shows projection for the 16A(78)-32 well.

In the most recent phase of activity at Utah FORGE a deviated well was completed in February 2021 and stimulation of the toe of this well occurred during April 2022. This stimulation again occurred in three stages, but with larger volumes (~660 m^3, ~450 m^3, and ~300 m^3) and at higher injection rates. Seismic monitoring for this phase was more extensive consisting of multiple deep boreholes along with the local seismic network (Rutledge et al., 2021) and a 210-surface nodal geophone array. As additional experiments are performed at Utah FORGE, revisiting the seismic data from completed stimulations can inform future operations. In this study, we revisit the microseismic response from the 2019 stimulation using a new matched filter enhanced seismic catalog (Dzubay et al., 2022) to better estimate and compare to the 2022 stimulation.

2. Data

In this study we utilize an enhanced seismic catalog for the 2019 stimulation (Dzubay et al., 2022). Dzubay et al. (2022) implemented a matched-filter detector using template microseismic events from the 2019 stimulation recorded at seismic station FORK (sensors located in ~30 meter deep borehole 68-32 about 120 meters NNE, Figure 1.). Starting with 12 events identified in the Schlumberger catalog, 133 unique events (M -1.8 to -0.1) were added to the catalog, bringing the total up to 534 events. The majority of these events, including one of the largest, occurred after the completion of the stimulation. The remainder of events occur both during and in between injection phases. The combined catalog together with cumulative injected volume and total pump rate for the first two injection stages are shown in Figure 2. Note that seismic events occurred in a swarm-like behavior some hours after an injection. The swarm with the most events occurs during the zone 2 stimulation on 4/27/2019 after a period of rapid cumulative volume growth from several consecutive pulses. Using this expanded catalog Dzubay et al. (2022) calculated a preferred b-positive value (van der Elst, 2021) of 1.61, which describes the relative abundance of larger to smaller magnitude earthquakes. Gutenberg-Richter b-values and b-positive are influenced by a variety of different factors, including rock type, stress state, and preexisting structures, and are used in relations estimating maximum magnitudes for induced events (e.g. van der Elst et al., 2016).

Table 1: Values of volume injected, maximum observed magnitude, and number of events by injection stage and cumulatively

Zone	Cycles	Volume [m^3] In Increment	Cumulative Volume [m^3]	Maximum Magnitude [M_w] In Increment	Cumulative Maximum Magnitude [M_w]	Number of Events In Increment	Cumulative Number of Events
1	1, 2, 3, 4	5.4	5.4	-1.5	-1.5	2	2
1	5, 6, 7	20.3	25.7	-0.7	-0.7	20	22
1	8, 9	45.4	71.1	-0.7	-0.7	34	56
Intermission		0	71.1	-0.1	-0.1	5	61
2	1	0.3	71.4	-0.8	-0.1	8	69
2	2, 3, 4	5.5	76.9	-1.3	-0.1	11	80
2	5, 6, 7, 8	53.4	130.3	-0.5	-0.1	236	316
2	9	29.8	160.1	-0.5	-0.1	70	386

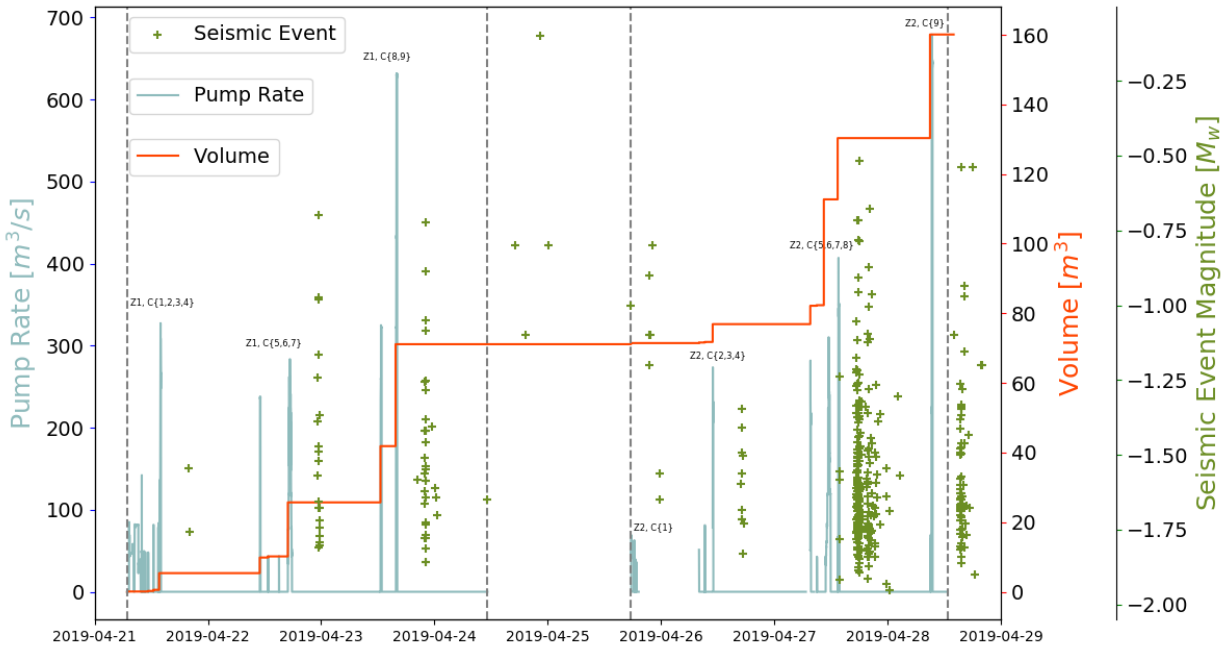

Figure 2: Seismic events (green crosses) shown in relation to injection pump rate (blue) and cumulative volume (red) for Zone 1 (2019-04-21 to 2019-04-24) through Zone 2 (2019-04-25 to 2019-04-29).

3. Analysis

3.1 Maximum Magnitude Estimates

We use two established relationships to estimate the maximum expected magnitude, McGarr (2014) and van der Elst et al. (2016). The McGarr (2014) relation limits the maximum magnitude to be the product of the injected volume and the shear modulus μ. The van der Elst et al. (2016) relation combines the Gutenberg-Richter parameter comparing an earthquake sequence's distribution of high magnitude events to low magnitude events (b-value) and the seismic potential of a given fluid injection (seismogenic index, ∑, Shapiro et al. 2010). Both b-value and ∑ are region specific. We modify the van der Elst et al. (2016) relation by using b-positive (van der Elst, 2021) and calculate a maximum magnitude as the injection progresses versus the maximum magnitude for the total volume of injection. Figure 3 shows the observed maximum magnitude for stages 1 and 2 of the 2019 stimulation compared to estimated maximum magnitudes using the relation defined in McGarr (2014) and van der Elst et al. (2016). For implementing the van der Elst et al. (2016), we set the b-value to 1.61 (Dzubay et al., 2022) and vary ∑. We can see in Figure 3 that the largest event to occur in zones 1 and 2 (a M_w = -0.1 event) is well below the McGarr threshhold and indicates a seismogenic index of ∑≤-2.

In Figure 4 a) and c) we plot the magnitudes of the largest events to occur in every injection cycle group against both cumulative volume and the cycle group's volume. There is no observable linear trend to these data.

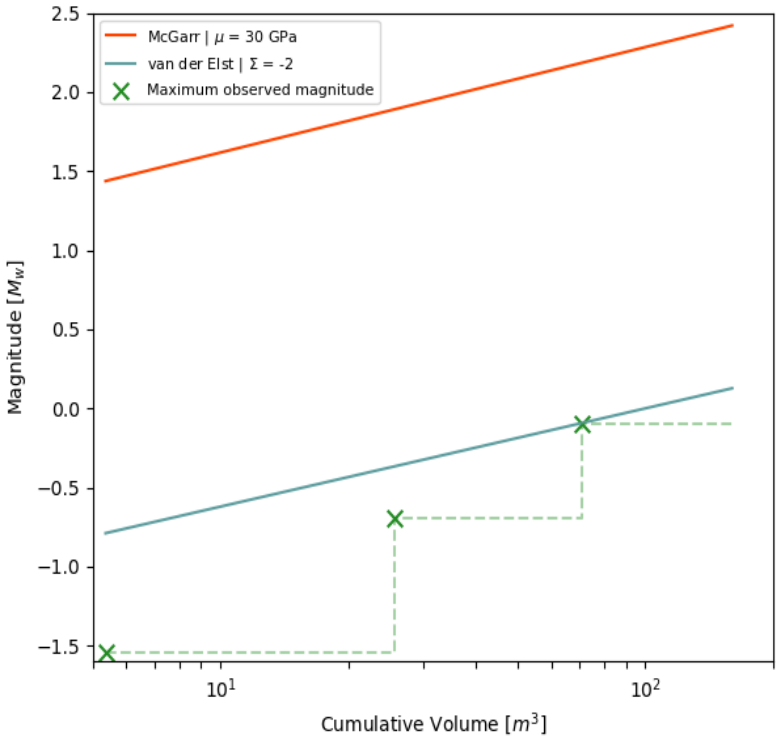

Figure 3: The McGarr and van der Elst relations for maximum expected magnitude with the maximum observed magnitude from zones 1 and 2 of the 2019 FORGE stimulation.

3.2 Number of Events

An additional parameter important for characterizing the microseismcity is the estimated number of detectable events. In Figure 4, we plot the total number of events for the first two stages with the injected volume of incremental injection cycles and also with the cumulative injected volume. There appears to be a linear trend visible in Figure 4 b) and d) that indicates the number of events grows with increasing injection volume. However, this linear trend is not consistent between zones 1 and 2. Zone 2 has several times more events per unit of injected volume than zone 1.

If we look at zones 1 and 2 from the 2019 injection, we find an average of 2.4 events per m^3 of fluid injected. This differs from what was observed for the 2006 Basel EGS stimulation where an average of 0.2 events occurred per m^3 of injected fluid (Bradshaw et al., 2022), which may be explained by differences in the stimulated rock volume or detection threshholds.

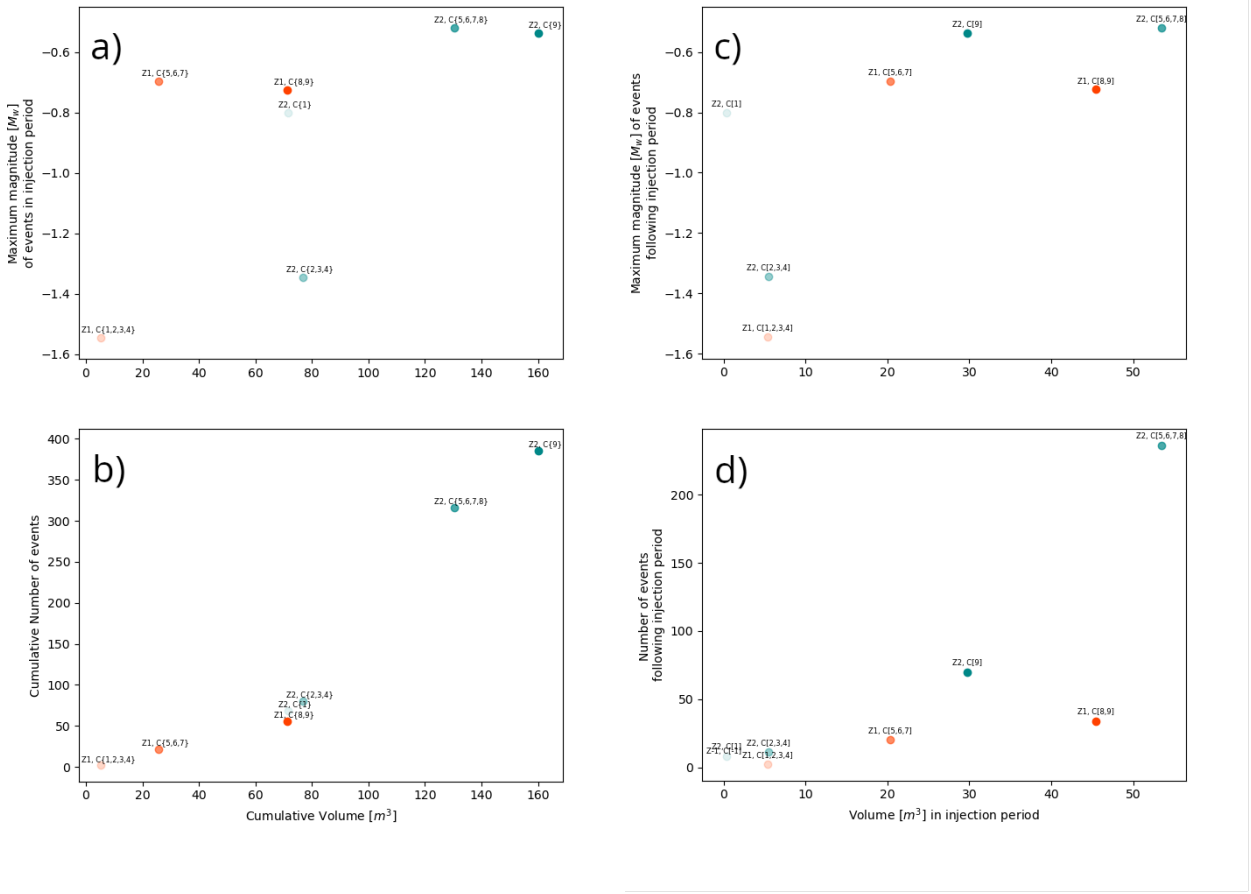

Figure 4: Maximum magnitudes and number of events for the zones 1 (orange) and zone 2 (blue) of the 2019 stimulation. The color intensity indicates earlier (lighter) to later (darker) injection cycles. a) The magnitudes of the largest events following each injection cycle grouping (labeled in Figure 2) against cumulative volume. b) The total number of detected events that occurred while injected against a cumulative volume. c) The magnitudes of the largest events in each injection cycle grouping against volume injected in the cycle grouping. d) The number of events to occur in each injection cycle grouping against the cycle grouping's injection volume.

3.3 First-Motion Focal Mechanisms

In characterizing the 2019 microseismicity, we are using HASH (Hardebeck and Shearer, 2002, 2003) to determine first-motion focal mechanisms. For this analysis, we are exploiting data collected from a surface geophone deployment (Figure 5). The array consists of 152 Fairfield Z-land 3 component geophones. For events with high signal-to-noise ratios recorded across a wide azimuthal band, we are measuring first motion directions and are exploring the inclusion of S/P amplitude ratios.

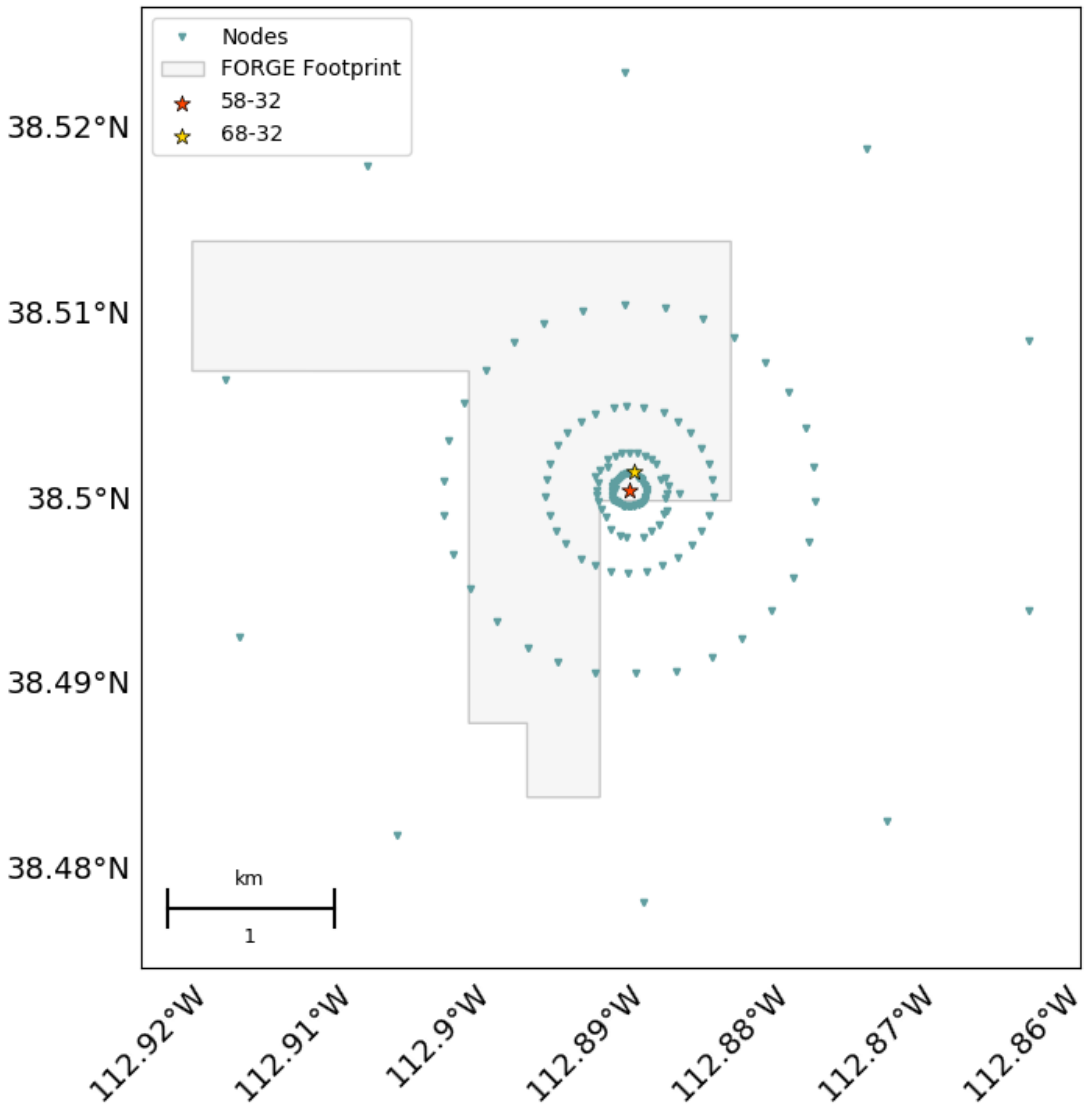

Figure 5: Nodal geophone deployment during the 2019 stimulation. Each blue triangle is a nodal seismometer. 58-32 (red star) is the stimulated borehole and 68-32 (yellow star) is the instrumented borehole.

4. Conclusions

Using the enhanced earthquake catalog for the 2019 stimulation (Dzubay et al., 2022), we examine the largest events and compare their magnitudes to what models predict. We find that the observed maximum magnitude is well below what was estimated by the McGarr (2014) relation. However, if we incorporate a region-specific b-positive value and constrain the seismogenic index to be -2, we find that the maximum observed magnitude of -0.1 is in agreement with an estimate using the van der Elst et al. (2016) relation.

We see a general trend of an increasing number of events with increasing cumulative injected volume. The seismic events associated with all injection cycles tend to occur in swarms delayed in time from the injections some hours after pumping. In general, a linear relation between the injected volume and the number of events would imply a more or less homogeneous and isotropic injection reservoir (van der Elst et al., 2016). These assumptions are broken by local variation in stress transfer or stress regime, heterogeneities like pre-existing faults, aseismic slip, and variable responses of opening fractures to injected volumes and therefore may result in a lack of correlation (e.g. discussions in De Barros et al. 2019, Niemz et al. 2020, Schoenball et al., 2020). In our study we see a linear increase in the number of events with cumulative injected volume in the cycles conducted in the first zone followed by a rapid increase in the number of events during the injections in the second zone. The change in seismic response may be attributed to reaching a critical cumulative injected volume or to mechanical differences between zone 1 and zone 2, as they refer to different locations along the borehole. Observations suggest that parameters in addition to injected volume are needed when examining the number of events in an injection-induced sequence. Practical mechanisms and parameters influencing the number of observed events are the focus of future research.

Acknowledgement

Funding was provided by The U.S. Department of Energy's Office of Energy Efficiency and Renewable Energy (DOE EERE) Geothermal Technologies Office under Project DE-EE0007080 Enhanced Geothermal System Concept Testing and Development at the Milford City, Utah Frontier Observatory for Research in Geothermal Energy (FORGE) site.

REFERENCES

Bradshaw, P.,Dyer, B., Bethmann, F., Dzubay, A., Petersen, G., Meier, P., and Pankow, K. (2022). Using the 2006 Basel enhanced geothermal systems project as a proxy for predicting reservoir development at Utah FORGE , 2022 Annual Seismological Society of America Meeting, Bellevue, WA, April 10-23, 2022.

De Barros, L., Cappa, F., Guglielmi, Y. *et al.* Energy of injection-induced seismicity predicted from *in-situ* experiments. *Sci Rep* **9,** 4999 (2019).

Dzubay, A., M. Mesimeri, K. M. Whidden, D. Wells, and K. Pankow (2022). Developing a comprehensive seismic catalog using a matched-filter detector during a 2019 stimulation at Utah FORGE: *Proceedings, 47th Workshop on Geothermal Reservoir Engineering*, Stanford University, CA February 7- 9, 8 p.

Hardebeck, J. L. and Shearer, P. M. (2002). A new method for determining first-motion focal mechanisms, *Bull. Seis. Soc. Am.*, 92, 2264-2276.

Hardebeck, J. L. and Shearer, P. M. (2003). Using S/P amplitude ratios to constrain focal mechanisms of small earthquakes, *Bull. Seis. Soc. Am.*, 92, 2264-2276.

McGarr, A. (2014). Maximum magnitude earthquakes induced by fluid injection. *Journal of Geophysical Research: Solid Earth, 119*(2), 1008-1019.

Moore, J., J. McLennan, R. Allis, K. Pankow, S. Simmons, R. Podgorney, P. Wannamaker, and W. Rickard (2019). The Utah Forntier Observatory for Researchin Geothermal Renergy (FORGE): An international laboratory for enhanced geothermal system technology development: *Proceedings, 44th Workshop on Geothermal Reservoir Engineering*, Stanford University, CA February 11- 13, 12 p.

Moore, J., J. McLennan, K. Pankow, R. Podgorney, S. Simmons, P. Wannamaker, C. Jones, W. Rickard, B. Barker, C. Hardewick, and S. Kirby (2020). Overview of Utah FORGE results in 2019: *Proceedings, 45th Workshop on Geothermal Reservoir Engineering*, Stanford University, CA February 10- 12, 10 p.

Niemz, P., Cesca S., Heimann S., Grigoli F., von Specht F., Hammer C., Zang A., Dahm T., Full-waveform-based characterization of acoustic emission activity in a mine-scale experiment: a comparison of conventional and advanced hydraulic fracturing schemes, *Geophysical Journal International*, Volume 222, Issue 1, July 2020, Pages 189–206

Pankow, K., M. Mesimeri, J. McLennan, P. Wannamaker, and J. Moore (2020). Seismic monitoring at the Utah Frontier Observatory for Research in Geothermal Energy: *Proceedings, 45th Workshop on Geothermal Reservoir Engineering*, Stanford University, CA February 10- 12, 9 p.

Rutledge, J**.,** K. Pankow, B. Dyer, P. Wannamaker, P. Meier, F. Bethmann, and J. Moore (2021). Seismic monitoring at the Utah FORGE EGS site, *GRC Transactions*, ***45***, 13 pp.

Schoenball, M., Ajo-Franklin, J. B., Blankenship, D., Chai, C., Chakravarty, A., Dobson, P., et al. (2020). Creation of a mixed-mode fracture network at mesoscale through hydraulic fracturing and shear stimulation. Journal of Geophysical Research: Solid Earth, 125.

Shapiro S., Dinske C., Langenbruch C., Wenzel F.; Seismogenic index and magnitude probability of earthquakes induced during reservoir fluid stimulations. *The Leading Edge* 2010;; 29 (3): 304–309.

van der Elst, N. J., B-positive : A Robust Estimator of Aftershock Magnitude Distribution in Transiently Incomplete Catalogs. Journal of Geophysical Research: Solid Earth, 126(2), (2021).

van der Elst, N. J., Page, M. T., Weiser, D. A., Goebel, T. H. W., and Hosseini, S. M.. Induced earthquake magnitudes are as large as (statistically) expected. Journal of Geophysical Research: Solid Earth, 121(6), (2016), 4575–4590.